

## USE OF NEW DEVELOPMENTS OF ATTITUDE CONTROL SENSORS FOR THE MICRO SATELLITE *FLYING LAPTOP*

Matthias Waidmann, Christian Waidmann, Dominik Saile, Georg Grillmayer  
Institute of Space Systems, Universität Stuttgart, Stuttgart, Germany  
grillmayer@irs.uni-stuttgart.de

Viola Wolter  
Steinbeis Transferzentrum Raumfahrt, Gäufelden, Germany  
wolter@tz-raumfahrt.de

### ABSTRACT

The *Flying Laptop* is a micro-satellite currently under development at the Institute of Space Systems, Universität Stuttgart. The primary mission objective of the *Flying Laptop* is technology demonstration for the future projects of the Institute of Space Systems. Several attitude sensors, either in-house developed or from external companies with no previous flight heritage, are being used. Electronic boards and mechanical housings were designed for the GPS system, the fiber-optic gyros and the magnetic torquers. The GENIUS experiment aims to increase the GPS accuracy in orbit by using an ultra stable oscillator (USO) and includes attitude determination. The C-FORS fiber optic gyro is a commercial product developed for aviation. With the Micro Advanced Stellar Compass made by the Technical University of Denmark and the Magnetometer made by Zarm-Technik new developments, so far not flown, are integrated. All attitude sensors and actuators are connected to a field programmable gate array (FPGA). This kind of on-board computer offers a more accurate timing and parallel processing of the sensors' and actuators' signals. The paper focuses on the attitude sensors and actuators and their interfaces to the on-board computer.

### NOMENCLATURE

ACS	Attitude Control System
C-FORS	Commercial Fiber Optic Rate Sensor
CCD	Charge Coupled Device
CHU	Camera Head Unit
COTS	Commercial Off The Shelf
FLP	<i>Flying Laptop</i>
FOG	Fiber Optic Gyro
FPGA	Field Programmable Gate Array
GENIUS	GPS Enhanced Navigation Instrument for the Universität Stuttgart micro-satellite
I <sup>2</sup> C	Inter Integrated Circuit
IBIS	Integrated Bus for Intelligent Sensors
LIS	Lost In Space
MGM	Magnetometer
MGT	Magnetic Torquer
OBC	On-Board Computer
PCB	Printed Circuit Board
PCDU	Power Control and Distribution Unit
PPS	Pulse Per Second
RW	Reaction Wheel
SCLK	Synchronous Clock
SEU	Single Event Upset
STR	Star Tracker
SuS	Sun Sensor
USO	Ultra Stable Oscillator

μASC	Micro Advanced Stellar Compass
μDPU	Micro Data Processing Unit

### 1. INTRODUCTION

The *Flying Laptop* (Figure 1) is a 100 kg, three-axis stabilized micro-satellite currently under development at the Institute of Space Systems, Universität Stuttgart and is planned to be launched into a sun-synchronous, low earth orbit. The primary mission objective is technology demonstration [1]. For the attitude control system several new sensors and also in-house developed components are utilized.

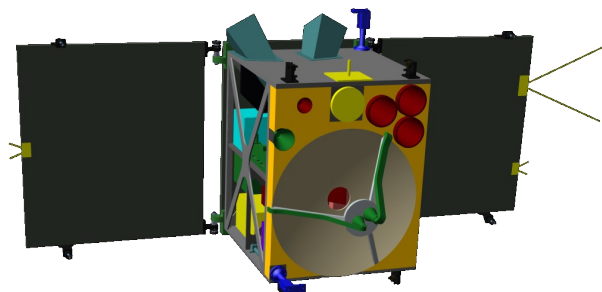


Figure 1: Flying Laptop

## 2. ACS DEVELOPMENT OVERVIEW

The satellite's motion is monitored by five different types of sensors: two three-axis magnetometers, two coarse sun sensors, four fiber-optic rate sensors, one autonomous star tracker with two camera heads and three GPS receivers. The actuators that rotate the satellite to the desired attitude are four reaction wheels and three magnetic torquers. All sensors and actuators are connected to the FPGA On-Board Computer (OBC) in a star like configuration. The ACS hardware devices are shown in Figure 2 and Figure 5, a more detailed description about the FPGA and the control algorithms is given in [2].

### 2.1 Operational Modes

The *Flying Laptop* uses different sensor/actuator combinations for several pointing modes as described in Table 1:

The objective of the **detumbling** mode is to reduce the angular velocity after launcher separation. An additional use is rate damping in case of accidentally exceeding the angular velocity limit.

The satellite is commanded to **safe mode** subsequent to the initial detumbling phase or in later mission phases whenever non-recoverable errors occur during pointing modes. The sensors for this mode need to have a high reliability, sensor outputs need to be available all the time but only a course pointing knowledge is required. Thus, only sun sensor and magnetometer information will be used. The commanded torque is realized with the help of the magnetic torque rods.

**Table 1: Operational Modes**

Mode	MGT	RW	MGM	SuS	STR	FOG	GPS
Detumbling	x		x				
Safe-Mode	x		x	x			
Inertial Pointing	x	x	x	(x)	x	x	
Nadir Pointing	x	x	x		x	x	x
Target Pointing	x	x	x		x	x	x

The **inertial pointing** mode will mainly be used for calibration and for technology demonstration of automated asteroid detection using the star tracker. A pointing stability of 150 arcseconds is required. Attitude and rate information is provided by the star tracker and the fiber optical rate sensors. Four reaction wheels are used for

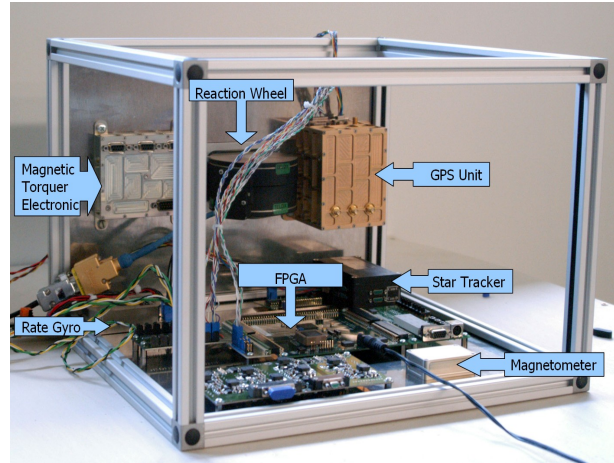


**Figure 2: "SpaceCube" for ACS Development**

actuation.

During earth observation in **nadir pointing** mode the satellite's body axes are aligned with the nadir coordinate system. The same type of non-linear controller with quaternion and rate feedback as for inertial pointing is used (the error quaternion now describes the error between body and nadir frame). The controller allows for large angle slew maneuvers to a nadir-pointed orientation from an arbitrary attitude and then stabilizes the satellite's nadir orientation within 150 arcseconds.

No earth referenced attitude is directly available from any sensor, but with the help of GPS data it is possible to transform the initial quaternions from the star tracker to the nadir frame. First the GPS-time is converted to JD2000 to calculate the Greenwich Mean Sidereal Time (GMST). From this, GPS position and velocity can be transformed from the earth-fixed to the earth-inertial frame.

In the **target pointing** mode the satellite remains aligned towards a fixed point on the earth's surface. This mode is mainly used for scientific investigations of the bi-directional reflectance distribution function (BRDF), off-nadir inspection of ground areas and during contact with the ground station using the high gain antennas. Suitable images for a BRDF target need to be taken along  $\pm 60^\circ$  pitch off nadir and within a maximum roll angle of  $\pm 5^\circ$ . An image with the payload cameras needs to be taken at every degree between the  $\pm 60^\circ$  during the flyover.

The controller for this mode is only slightly different from the one for nadir pointing. It uses quaternion and rate feedback as well but different setpoints for attitude and angular velocities. Star tracker, GPS and rate sensors will be used to precisely follow the calculated attitude profile within a pointing accuracy of 150 arcseconds.

## 2.2 ACS Algorithms

Figure 6 shows a global overview of the ACS algorithms. Each block shown represents a sub-function with inputs and outputs. On the left, inputs from the 5 sensors are shown representing the interface variables from the lower hardware dependent levels. The *Processing* section merges, converts and extrapolates the sensor variables to the current time and also contains the Kalman filters. In the *Navigation* part the reference attitude and reference angular velocity are calculated depending on the pointing mode selected. The *Control* section contains the safe mode, detumbling, desaturation, nullspace, inertial, nadir and target pointing controller [2]. For the last three an error quaternion feedback controller is used. The torque output from the controllers is scaled and processed in the *Command* section and sent to the wheels and magnetic torquers shown at the right hand.

## 2.3 ACS Algorithm Development Process

Figure 3 shows the development cycle for the ACS navigation and control algorithms. After initial theoretical analysis the algorithms are implemented in Matlab/Simulink and tested extensively for performance. All functions which are going to be implemented in the on-board computer are written as an embedded m-file. In the next step the algorithms have to be converted to Handel-C, which is a high level language compiler generating the binary netlist for the FPGA. Control algorithms and filters contain a large amount of calculations which require a large amount of gates in the FPGA. In order to limit the space needed on the FPGA almost all variables are converted to fixed point arithmetic and the outputs of the optimized algorithms is compared to the original double precision algorithms. The comparison is still performed in the Matlab/Simulink environment and is identical to the approach used for digital signal pro-

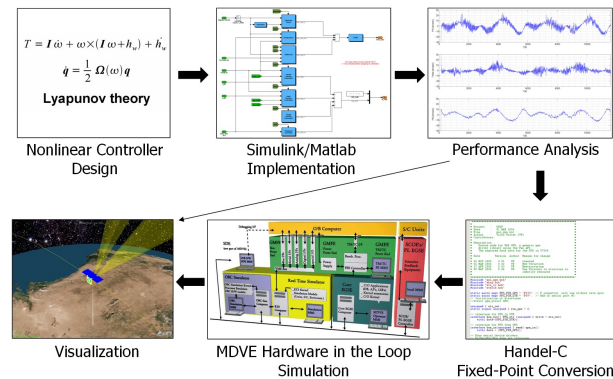


Figure 3: ACS Development Process

cessors. After compilation the netlist is loaded to a prototype FPGA board (Figure 2) for initial testing. For final verification of the algorithms a real time simulation environment is needed. A model-based system-simulation environment represented by the MDVE (Model-based Development and Verification Environment) is used.

## 3. GENIUS GPS SYSTEM

GPS is a commonly used sensor for satellites in low earth orbit in order to determine the position and velocity. This experiment will test the advanced usage of GPS for orbit navigation.

GENIUS was developed to serve two purposes. The first is the standard supply of real-time position and velocity data for on-board usage during nadir and target pointing. A precision of 10 m in position, 0.1 m/s in velocity and 1  $\mu$ s in time is envisaged using an internal orbit propagator and the possibility of uploading two line elements. The system is composed of three independent receivers, thus it assures a high level of redundancy for GPS on-board navigation. The second, innovative task is an experiment conducted in cooperation with the DLR/GSOC (German Space Operations Center) for accurate determination of the spacecraft attitude. This will be accomplished by the ground analysis of the measured GPS carrier phase of each receiver that is recorded on the satellite and dumped during ground station contacts. An accuracy of 0.1° to 1° is envisaged. Furthermore due to the use of an ultra stable time base navigation solutions with less than 4 tracked satellites can be studied, considering the future use of GPS in higher altitude orbits.

### 3.1 System Design Overview

Each of the three Phoenix GPS receivers is connected to

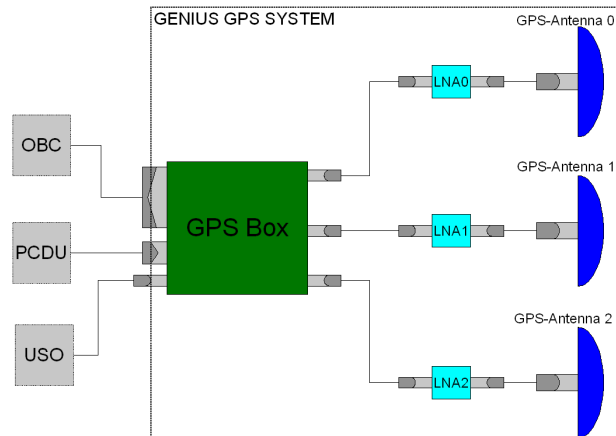
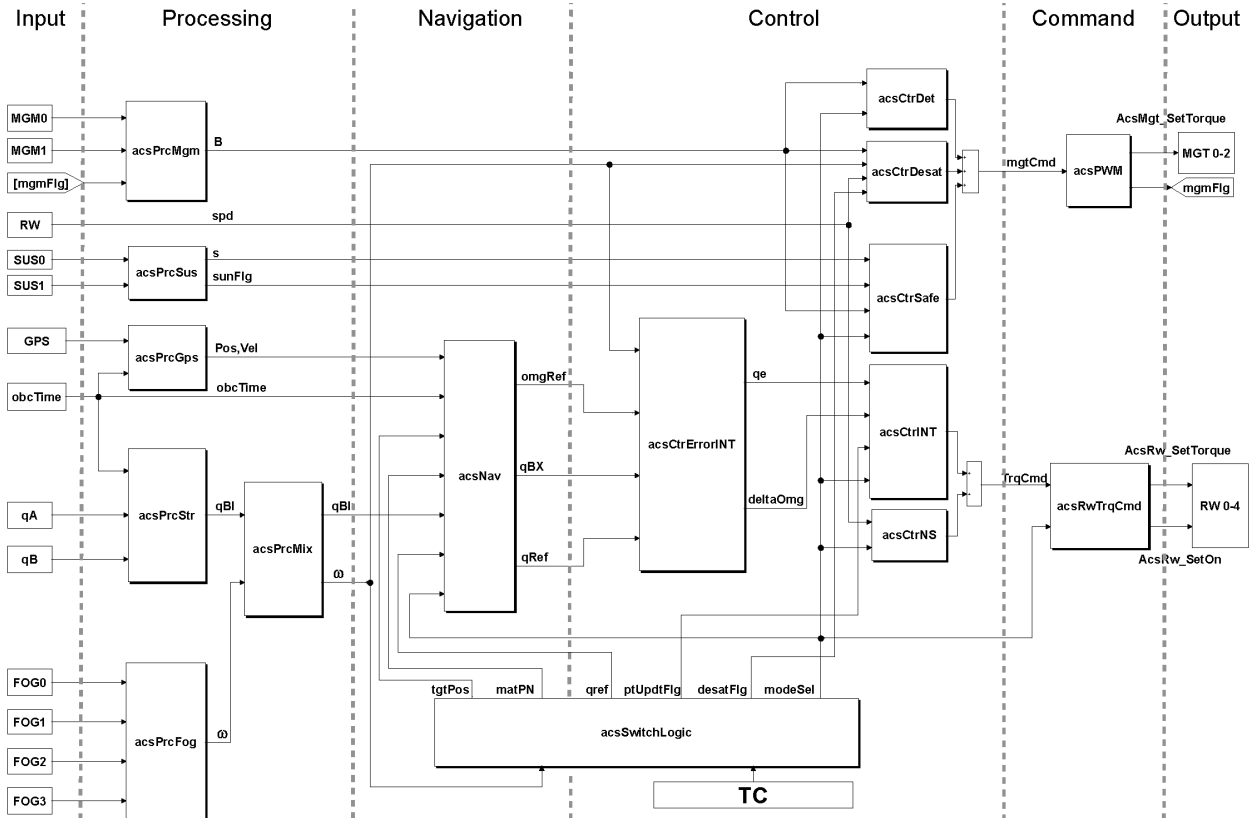


Figure 4: GPS Block Diagram



**Figure 5: Overview of ACS Sensors and Actuators**



**Figure 6: ACS Subfunction Map**

a separate GPS antenna and low noise amplifier as shown in Figure 4. The three GPS receivers are integrated in one box together with an interface board (Figure 7). The three external connections are the on-board computer, the power control and distribution unit (PCDU) and the ultra-stable-oscillator (USO).

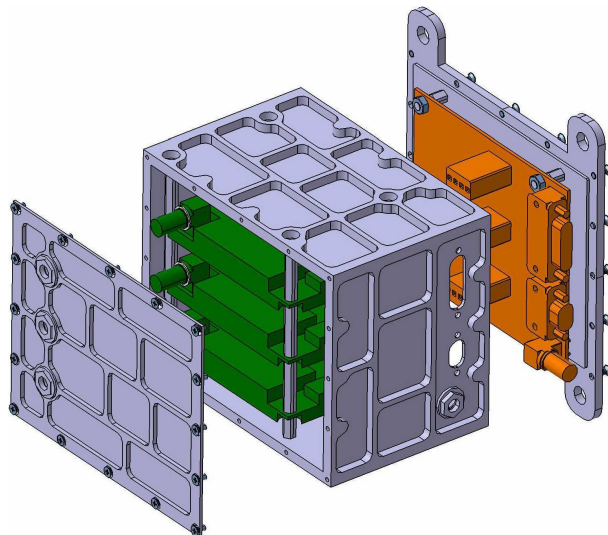


**Figure 7: GPS Modules**

The three antennas are placed on three corners of the satellite in an L-like arrangement, creating two baselines of 44 cm and 61 cm (Figure 8). This configuration is used to define the spacecraft attitude.

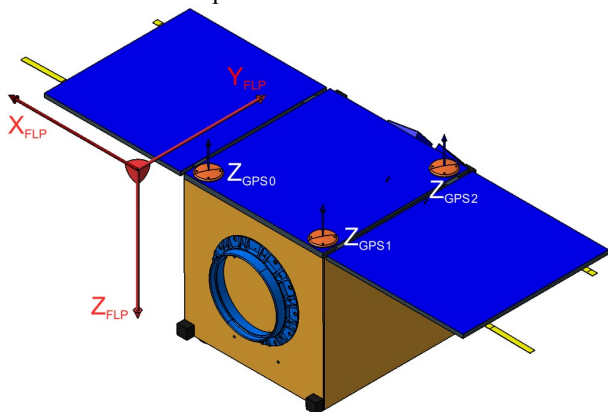


**Figure 8: GPS Antenna Arrangement on the Solar Panel.**

### **3.2 Phoenix GPS Receiver**

The Phoenix GPS receiver is a commercial GPS receiver board with a new DLR/GSOC developed firmware for space and high dynamics applications. The receiver has 12 tracking channels and is able to measure phase and Doppler shift of the GPS-L1 carrier signal. Several

modifications were made to prepare the receiver boards for space usage and to adjust them to the needs of the GENIUS system. The crystal oscillator of the GPS boards was removed since the time base for the GPS receivers is provided by an ultra-stable 10 MHz crystal oscillator (USO) on board the *Flying Laptop*. This way the receivers are synchronized for the carrier phase measurements.

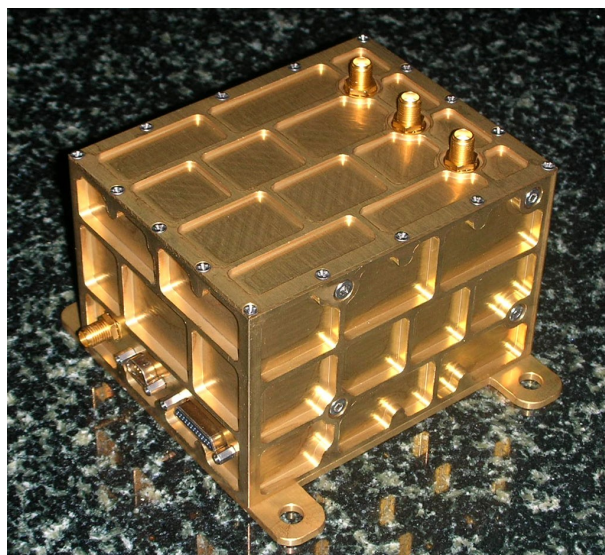


**Figure 9: GPS Hardware**

## **4. RATE SENSOR**

For the measurement of the angular rate, the micro-satellite *Flying Laptop* is equipped with 4 single-axis COTS fiber optic rate sensors in a tetrahedron configuration.

### **4.1 Fiber Optic Rate Sensor**

The measurement principle of fiber optic rate sensors is based on the Sagnac effect. The used sensors C-FORS (Commercial Fiber Optic Rate Sensor, Figure 10) are produced for terrestrial and aeronautical applications by Litef. Due to the use of COTS parts, the sensor is much cheaper than space qualified rate sensors, but nevertheless its performance is similar to those used for space applications. Currently it is one of the most accurate rate sensors not subject to ITAR restrictions. By flying the sensor the space environment effects on the sensor are evaluated.

The C-FORS [3] is designed to survive shocks of up to 250 g (non-operating, 1 ms half-sine) as well as linear accelerations of up to 100 g and sine sweep vibrations with an amplitude of 1.5  $g_{RMS}$  in the frequency range of 5-2000 Hz. Therefore the sensor is expected to with-



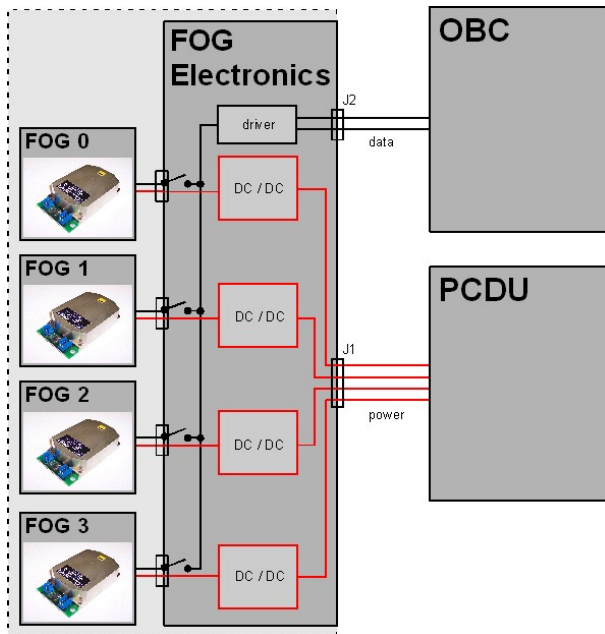


**Figure 11: Electrical Design Overview**

cluding the 4 sensors and an electronic unit (FOG electronics). Both, power supply and communication is independent for each FOG but placed together on this common electronic board.

A small interface board is soldered to the bottom side of each FOG (Figure 10) to provide a connector interface. The DC/DC converters and the signal driver mainly consist of commercial integrated circuits.

#### **4.4 Power Supply**

Due to the necessity of 4 independent sensors, each of the sensors is supplied separately by the Power Control and Distribution Unit (PCDU). To avoid a huge amount of wires and due to the exigency of switching all voltages simultaneously, only one voltage of +5.2 V is supplied 4 times by the PCDU. The operating voltages for each of the sensors (Table 3) are generated by DC/DC converters located on the common electronic unit as shown for one FOG in Figure 12. Each converter ensures the required voltage stability of all supply voltages for each FOG and a simultaneous switch on and off of the voltages.

#### **4.5 Data transmission**

The C-FORS provides both an asynchronous and a synchronous interface for communication.

The synchronous interface allows for a maximum data rate of 4 kHz, as opposed to a possible maximum data rate of 1 kHz for the asynchronous interface. Also, the

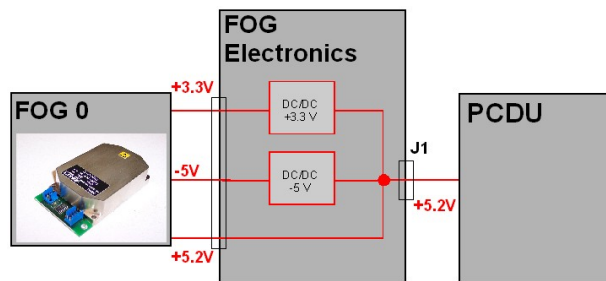


**Figure 12: Power supply of one FOG (data lines and ground not illustrated).**

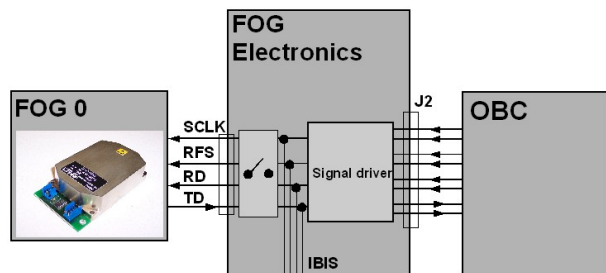


**Figure 13: Data lines between FOG and OBC (power supply and ground not illustrated)**

data request is issued to all four sensors at exactly the same time. Thus the data from each sensor is exactly synchronized to the OBC time. For this reason the common synchronous 4-wire IBIS bus is utilized (Figure 13). The SCLK line is used to issue a 2 MHz clock signal to each sensor. On the receive frame synchronization (RFS) line, a 500 ns pulse synchronization signal triggers the simultaneous generation of measurement data in each FOG every 256 clock cycles. The sensors are then read out sequentially following a preprogrammed scheme.

The IBIS lines of the FOGs are connected to the common bus on the electronic unit, where the ground asymmetric signals are converted into ground symmetric signals by a signal driver for transmission to the OBC. If any FOG is powered down, the sensor is disconnected from the IBIS by an analog switch. Thus, the bus is not affected by a defective and/or powered down FOG.

#### **4.6 Heat Dissipation**

The waste heat produced by the DC/DC-converters and the signal driver is dissipated via the mounting screws of the printed circuit board of the FOG electronics.

#### 4.7 Mechanical Design

The whole FOG-unit is shown in Figure 14 and within the satellite in Figure 15. It consists of the following main parts:

- Electronic box which is both mounting interface to the satellite and housing of the main electronic unit.
- Electronic unit;
- Base plate which is both cover for the electronic box and basis for the tetrahedron alignment of the FOGs;
- Ramps and a mounting plate for the assembly of the FOGs in tetrahedron configuration;
- FOGs including the interface board equipped with the interface connector;
- Shielding cases for reduction of the total radiation dose.

The system is currently being assembled. The calculated total weight is approx. 1.7 kg at the overall dimensions of 186 x 122 x 150 mm (LxWxH).

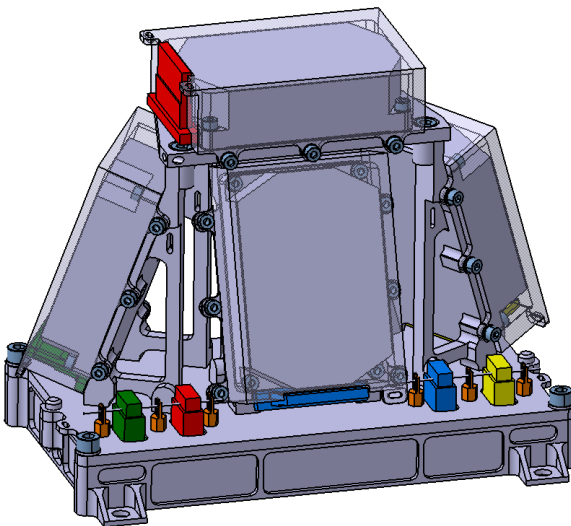


Figure 14: FOG Unit

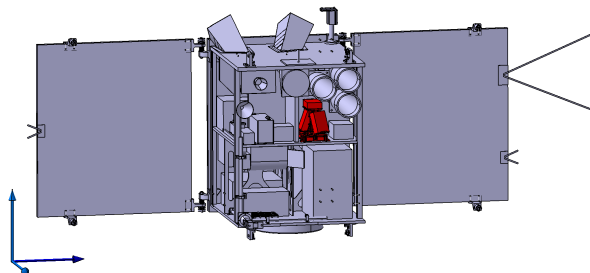


Figure 15: FOG Unit within the Micro-Satellite *Flying Laptop*

#### 5. STAR TRACKER

The star tracker is the most accurate attitude determination sensor on the *Flying Laptop*. The selected model is the micro-Advanced Stellar Compass ( $\mu$ ASC) of the Technical University of Denmark.

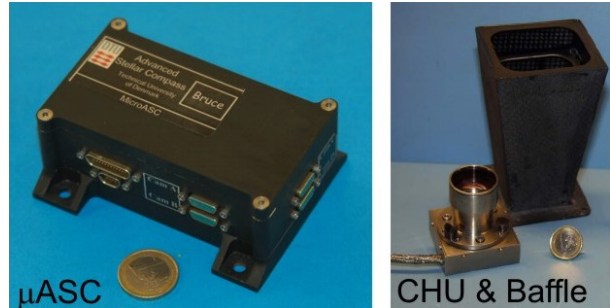


Figure 16: Micro-Advanced Stellar Compass (left) and Camera Head Unit & Baffle (right)

The  $\mu$ ASC is the successor of the Advanced Stellar Compass, which has been successfully used for more than 15 missions for ESA, CNES, NASA, DLR and NASDA. Its smaller size and lighter weight makes it a suitable device for micro-satellites like the *Flying Laptop*. So far it was not launched on a satellite.

The  $\mu$ ASC system (Figure 16) consists of 3 separate units; the micro-Data Processing Unit ( $\mu$ DPU), the Camera Head Unit (CHU) and the baffle system.

In normal operation, the  $\mu$ DPU creates a digital image of the acquired analogue data received from the CHUs every 0.5 s and stores it in the internal RAM. In further computing, the lens distortion is removed and the image is sifted for adequately bright objects. The amount of bright objects that are found in an image can be influenced by varying a software parameter, but should never be below 16 stars, which is the minimum to guarantee

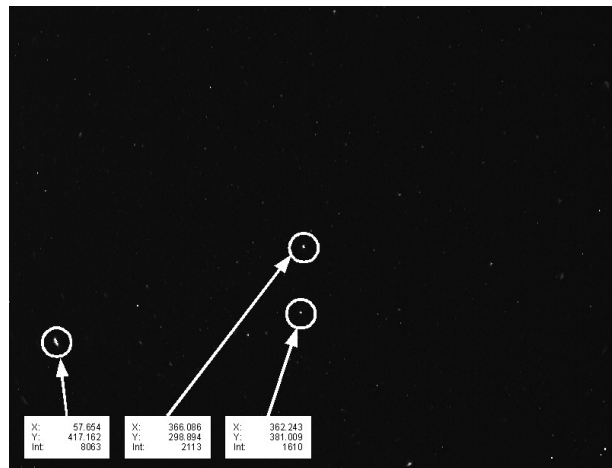


Figure 17: Image taken by the CHU with exemplary position and magnitude of three stars

reliable information. The developers recommend an amount of detected stars between 20 and 80. Up to 199 stars can be detected. The center and magnitude of each detected star is determined and stored in a list. Figure 17 shows a representative image where the position and magnitude of 3 stars is labeled. In normal operation, the stars are matched against the star catalog. It contains approximately the 12,000 brightest stars and is based on the Hipparcos catalog supplemented by Tycho II. If the match quality is within a defined threshold, the new attitude is found. Under the threshold, a further procedure, the Lost In Space (LIS) mode, is initiated automatically. In this mode, stars that are brighter than a certain value and their neighbours are compared to a separate star database to find a crude attitude. This database contains the attitude and distances between the 4,000 brightest stars and is used either to feed the normal operation algorithm, the initial attitude determination or helps to provide a coarse attitude in case of high rotation. The attitude is delivered to the OBC as quaternions in the heliocentric inertial equatorial reference frame J2000.0.

### 5.1 Camera Head Unit (CHU)

The CHU uses a CCD-chip with a size of 7.95 mm x 6.45 mm with 752 x 558 pixels to make images of the firmament. Stray light of bright objects like the sun, the earth and the moon that could interfere with the measurement is absorbed in the baffle system, which also reduces the field of view for each CHU to 13.4° x 18.4°.

While the  $\mu$ ASC is capable of supporting four CHUs, for the *Flying Laptop* a configuration of two CHUs was selected as a compromise between attitude availability on the one hand and available space and size (specially for the baffles) on the other hand.

### 5.2 Micro-Data Processing Unit ( $\mu$ DPU)

The data acquired by the CHUs is picked up by the  $\mu$ DPU to process the satellite's attitude. It is equipped with a 486 microprocessor and three types of memory; a

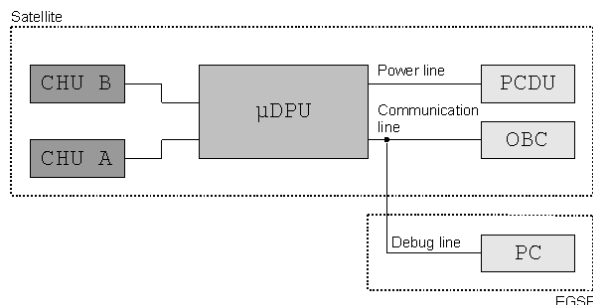


Figure 18:  $\mu$ ASC Interface Diagram

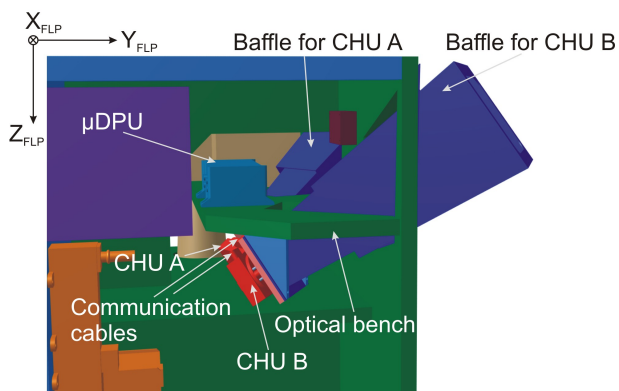


Figure 19: Integration of the Star Tracker System on the *Flying Laptop*

64 kB PROM , an 8 MB Flash and an 8 MB RAM.

### 5.3 Electrical Interface

As shown in Figure 18 the  $\mu$ DPU is connected to the on-board computer through a RS-422 interface with 115200 baud. The 20 V power supply is provided by the power control and distribution unit (PCDU). The nominal power consumption for the FLP configuration with two CHUs is 5 W. For ground tests, the  $\mu$ DPU can additionally be controlled by a PC over a special debug line.

### 5.4 Arrangement on the Satellite

Figure 19 shows the integration of the star-tracker system on the FLP. Both CHUs with corresponding baffles are placed on an optical bench and connected with the  $\mu$ DPU which is located on the other side of the bench.

To avoid blinding, an analysis for the angle between the boresight of the CHUs and the sun-earth axis has been conducted. The orientation of the CHUs has to be chosen in a way that the mentioned angle does not fall below the worst case sun exclusion angle of 55° and the

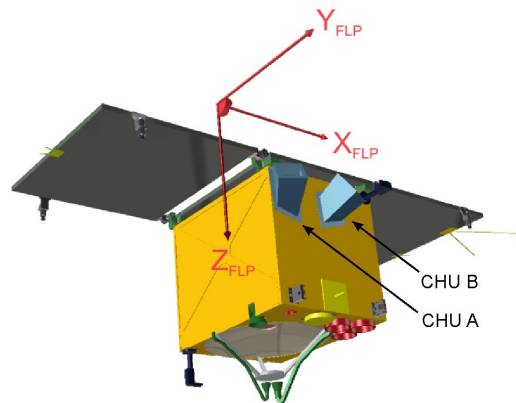


Figure 20: Orientation of CHUs and Baffles.

earth exclusion angle of  $25^\circ$  and that the system still fits into the already tightly packed satellite design. These studies have led to the following orientation of the CHUs with respect to the axes of the satellite:  $125^\circ$  elevation from the z-axis and  $45^\circ$  between the two CHUs (Figure 20). This orientation avoids blinding of the CHUs for most of the pointing maneuvers.

The baffles are optimized for earth proximity operations to maximize roll at the expense of the sun exclusion angle.

### 5.5 Accuracy

The  $\mu$ ASC allows the determination of the attitude within an accuracy of 1-2 arcseconds for an angular rate of less than  $0.025^\circ/\text{s}$  [4]. The accuracy is disturbed by various influences. The most obvious disturbance is caused by motion and rotation of the satellite that causes a smearing of some of the stars on the image or even moving them out of the FOV. The  $\mu$ ASC is much more sensitive to rotations across the boresight than around it: For an update rate of 0.5 s, the  $\mu$ ASC switches to the LIS mode for a rotation of  $4^\circ/\text{s}$  around boresight, whereas this mode is already reached for a rotation of  $0.4^\circ/\text{s}$  across boresight. A higher update rate allows higher angular rates but reduces integration time and thus accuracy. For highest accuracy 2 Hz update rate is recommended by the Technical University of Denmark.

Furthermore, precession and nutation of the earth cause deviations from the true attitude because the output quaternions are given in an equatorial system, leading to an error of about 5 arcseconds per year. Orbital aberration and annual aberration results from relativistic effects of fast movement of the satellite around the earth and the sun. The maximum displacement caused by annual aberration is 5.4 arcseconds in LEO. On the *Flying Laptop* it is possible to correct these effects by transmitting the GPS time and position to the star tracker.

Another error is caused by the inaccuracy of the internal clock of the star tracker. To minimize it, the clock is synchronized with the ultra-stable on-board computer clock every 10 seconds.

## 6. MAGNETOMETER

The satellite is equipped with two 3-axis anisotropic-magneto-resistive (AMR) magnetometers manufactured by Zarm-Technik. It is a new development that was initiated by the *Flying Laptop* project.

The measured vector of the earth's magnetic field is used as input information for the magnetic torquers, for detumbling after launcher separation, rate damping in case of accidentally exceeding the angular velocity limit



Figure 21: AMR Magnetometer

and desaturation of the momentum wheels.

An integrated three-axis AMR sensor HMC-1023 from Honeywell measures the magnetic field in three directions [5]. For each direction, an independent permalloy bridge is used for magnetic measurement. The output is linear proportional to the applied magnetic field. The analogue sensor output voltage is converted into a digital value by a sigma delta A/D-converter. The magnetometer temperature is monitored by a temperature sensor that is also used for temperature compensation. A micro-controller handles the communication between user and sensors. The magnetometer is encased by a housing consisting of 2 to 3 mm aluminium alloy.

### 6.1 Magnetometer Interface

The magnetometer is connected to the on-board computer by a RS-422 interface with 57 600 baud. A micro-D connector is used on the magnetometer for communication and 5 V (0.082 W) power supply.

After each data request a response message, containing 2 bytes of data for each direction and additional 2 bytes for the temperature, is transmitted to the on-board computer. The magnetometer runs in *fast* mode using an integration time of 167 ms, but data is requested only every 5 s when the magnetic torquers are shut off.

The sensor sensitivity is about 8.5 nT. The A/D-converter resolution is 16 bits, which is equal to 5 nT for the last significant bit. The measurement range is  $\pm 150 \mu\text{T}$ . The manufacturer states an accuracy of  $< \pm 1\%$ .

## 7. MAGNETIC TORQUER

Three ZARM-Technik magnetic torquers (torque rods) with a linear dipole moment of  $6 \text{ Am}^2$  are utilized. The torquers are connected to a power switch that is commanded by two independent I<sup>2</sup>C buses from the OBC (Figure 22). The magnetic torquer system is essential to the satellites functioning and thus the whole system is

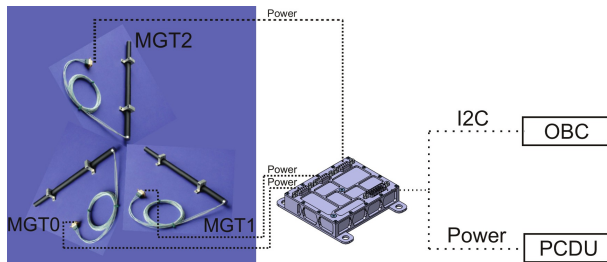


Figure 22: MGT Block Diagram

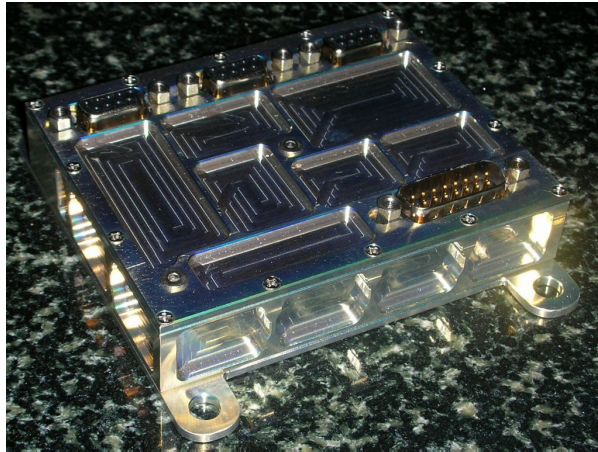


Figure 23: Magnetic Torquer Power Electronics

fully redundant.

The power electronics contain an H-bridge supplying the torquers with either 5V, -5V or switched off (bang-bang actuation). The torquers are pulse-width-modulated and commanded by the acsPWM subroutine in the ACS controller via the I<sup>2</sup>C interface. Again, to reduce mass the pockets of the aluminium case are milled out as shown in Figure 23.

## 8. SUN SENSORS

The sun sensors system consists of two three-axis Coarse Sun Sensors from Sun Space mounted at diagonal corners of the satellite. The sensor's voltages are digitized and sent to the OBC via two I<sup>2</sup>C buses.

## 9. REACTION WHEELS

Four reaction wheels RSI 01-5/28 made by Teldix are running in a single hot redundant tetrahedron configuration with nullspace control. Each of the wheels has an angular momentum capacity of 0.12 Nms and a reaction torque of 5 mNm over the range of  $\pm 3000$  rpm. The reaction wheels are connected to the on-board computer via a RS-422 interface at 9600 baud.

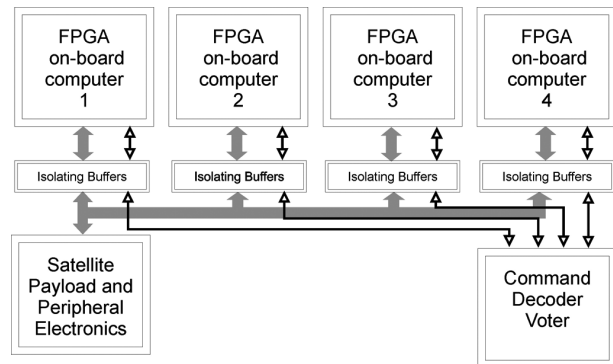


Figure 24: OBC Block Diagram

## 10. ON-BOARD COMPUTER

The on-board computer (OBC) of the *Flying Laptop* is a new development based on field programmable gate arrays (FPGAs). The OBC computer consists of four FPGA nodes (Figure 24), each of which can act as the master OBC. The quadruple redundancy is necessary to handle radiation as the individual nodes are not radiation hard. The master OBC is selected by a radiation hardened command decoder and voter (CDV).

The FPGA OBC nodes are programmed with Handel-C, a programming language similar to C, developed especially for FPGAs. Handel-C allows programming in the high-level-language style with the additional feature of direct hardware manipulation.

### 10.1 Sensor Control by the FPGA

All sensors and actuators are connected to the OBC. Each of the four FPGA nodes is able to listen to signals from the sensors. Only the master node is allowed to send commands. If a restart of a node is necessary, e.g. caused by a single event upset (SEU), it can synchronize itself to the other nodes by listening to the signals from the sensors and through synchronization signals between the nodes.

The use of FPGAs allows the implementation of many kinds of interfaces directly in the FPGA. Asynchronous as well as synchronous communication is possible, binary signals like clocks can be issued with only minor limitations. Since most of the attitude control sensors and actuators are designed for the use with micro-processor systems, serial communication is the most common interface. It is used by the GPS, the reaction wheel, the magnetometer and the star tracker. For the fiber optic gyro synchronous serial communication is chosen. For sensors and actuators that require only simple and low amount of data communication, the I<sup>2</sup>C Bus was selected like for the magnetic torquers and sun sensors.

## **10.2 FPGA Advantages**

When serial communication is used for the sensor control, the speed is mostly determined by the serial baud rate and the response time by the sensors. With the FPGA real parallel transmission, reception and processing of the many interfaces is possible.

Another advantage of programs running in hardware is the time stability. When telemetry is received from the sensors, the time for the processing of the message is always exactly the same (no interrupts like for micro-controllers) and can also be pre-calculated as a function of the OBC internal clock rate.

The GPS and the star tracker are the only devices that do not require a data request or command, but send their telemetry individually and not in sync to the ACS control cycle. The GPS therefore sends a PPS synchronization signal every second. The star tracker on the other is synchronized directly with a PPS signal every 10 seconds. Having always a constant processing time directly results in no time variation and thus the best available navigation accuracy.

## **11. CONCLUSIONS**

The attitude control system contributes to the main purpose of the *Flying Laptop*, technology demonstration, by using new developed components and COTS devices. The critical components are redundant as a safeguard against unpredicted failures. New concepts like the GENIUS GPS system and the FPGA on-board computer are used to increase the overall performance of the attitude control system.

## **REFERENCES**

- [1] Grillmayer, G., Falke, A. and Roeser, H.P., "Technology Demonstration with the Micro-Satellite Flying Laptop", Selected Proceedings of the 5th IAA Symposium on Small Satellites for Earth Observation, Berlin, Germany, 4-8 Apr. 2005, pp. 419-427.
- [2] Grillmayer, G., Hirth, M., Huber, F., Wolter, V., "Development of an FPGA Based Attitude Control System for a Micro-Satellite", AIAA-2006-6522, AIAA/AAS Astrodynamics Specialist Conference, Keystone, CO, USA, 21-24 Aug. 2006.
- [3] Litef GmbH, "Specification of the Litef C-FORS fiber-optic gyroscope", 144410-0000-312, Rev. B, 2005.
- [4] Technical University of Denmark, "micro-Advanced Stellar Compass User's Manual", IRS-DTU-MA-3001, Issue 1.1, 2005.

- [5] Zarm-Technik GmbH, "Magnetometer Manual (MM)", IRS-ZAR-MAG-MM-01-0001, Issue 1, 2006.